

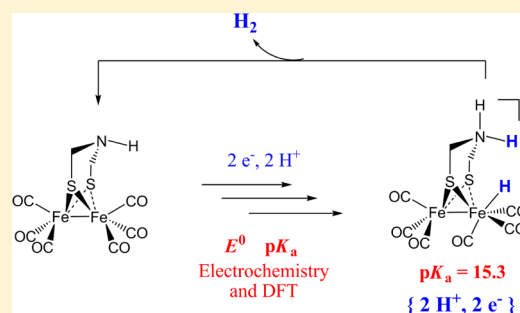
Mechanistic Insights into the Catalysis of Electrochemical Proton Reduction by a Diiron Azadithiolate Complex

Marc Bourrez,^{*,†} Romain Steinmetz,[†] and Frederic Gloaguen^{*,†}

[†]UMR 6521, CNRS, Université de Bretagne Occidentale, Brest, France

S Supporting Information

ABSTRACT: Cyclic voltammetry experiments and DFT calculations allowed us to establish a complete mechanism of the catalysis of electrochemical proton reduction by $[\text{Fe}_2(\mu\text{-SCH}_2\text{N}(\text{H})\text{CH}_2\text{S})(\text{CO})_6]$ (Fe–adt) in acetonitrile. The proposed mechanism is fully consistent with the observed dependence of the voltammetric responses on the strength of the acid used as a proton source. Addition of moderately strong acids, such as $\text{CCl}_3\text{CO}_2\text{H}$ ($\text{p}K_a = 10.7$) or $\text{HOTs}\cdot\text{H}_2\text{O}$ ($\text{p}K_a = 8.6$), triggers the occurrence of new reduction events at potentials less negative than the reduction of Fe–adt, therefore ascribed to reduction of the protonated forms of the complex. Reduction of the N-protonated form seems to favor a tautomerization reaction leading to a Fe–H intermediate. On the other hand, addition of weak acids, such as $\text{ClCH}_2\text{CO}_2\text{H}$ ($\text{p}K_a = 15.3$), leads to direct protonation on the diiron site subsequently to reduction of the catalyst. A better understanding of the mechanism of proton reduction by the biologically relevant Fe–adt derivative could impact the design of improved catalysts inspired by FeFe–hydrogenase.



INTRODUCTION

There is growing interest in the development of molecular systems capable of producing molecular hydrogen (H_2) from electrochemical and photochemical water splitting.^{1–3} Oxidation (or combustion) of H_2 releases a large amount of energy, giving water as the only reaction product. H_2 is also a strong reducing agent, which can be used in the synthesis of liquid fuels either directly from carbon dioxide (CO_2)^{4,5} or from carbon monoxide (CO)^{6,7} obtained through fixation of CO_2 .^{8–12} On the other hand, some microorganisms produce H_2 in the course of their normal metabolism. This process involves an enzyme called FeFe–hydrogenase (FeFe– H_2 ase) that achieves a turnover frequency (TOF) exceeding 6000 s^{-1} at a potential close to the thermodynamic limit.^{13,14} Activation of protons by the FeFe– H_2 ase occurs at a diiron subsite, in which the Fe atoms are coordinated to CO and CN^- ligands and linked by a dithiolate bridge of the type $-\text{SCH}_2\text{XCH}_2\text{S}-$ (Scheme 1).^{15,16} The nature of the central group X has been a matter of debate for many years. However, recent studies combining spectroscopy and synthesis of artificial FeFe– H_2 ase have provided strong evidence that the bridging ligand is actually an azadithiolate (adt, $-\text{SCH}_2(\text{NH})\text{CH}_2\text{S}-$).^{17–20} This amine group is thought to serve as a proton shuttle to the diiron center, “favoring” thus catalysis of proton reduction. However, it remains to be established whether this favorable role is thermodynamically or kinetically controlled. Indeed, the protonated form adt-NH^+ can assist the transfer of H^+ to Fe via a tautomerization reaction and/or stabilize the hydride Fe–H through hydrogen bonding,²¹ facilitating subsequent formation and release of H_2 (Scheme 2).^{22,23} Furthermore, a

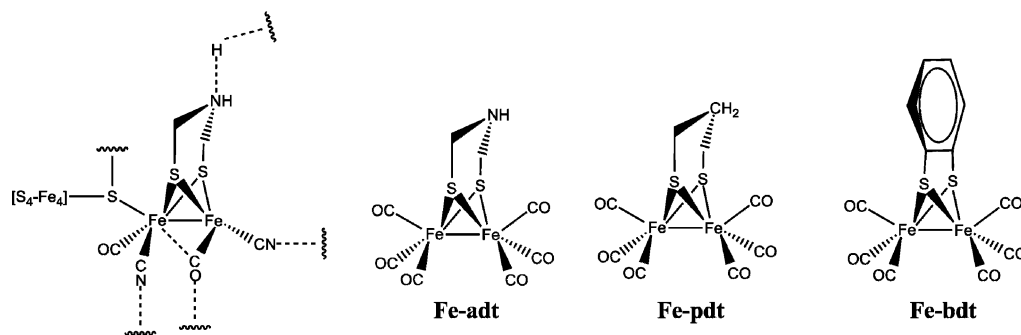
concerted proton–electron transfer may occur at some point.^{24–27}

Although the electrochemistry of FeFe– H_2 ase models has been extensively investigated,^{28–34} few detailed studies of complexes with a dithiolate bridge bearing a tertiary amine group ($-\text{SCH}_2\text{N}(\text{R})\text{CH}_2\text{S}-$) have been reported^{35–40} and none concerning the biologically relevant adt bridge. Catalytic reduction of strong acid ($\text{HBF}_4\cdot\text{Et}_2\text{O}$, $\text{p}K_a < 2$ in MeCN) by $[\text{Fe}_2(\mu\text{-SCH}_2\text{N}(\text{R})\text{CH}_2\text{S})(\text{CO})_6]$ ($\text{R} = \text{CH}_2\text{CH}_2\text{OCH}_3$, $E_{1/2,\text{red}} = -1.6\text{ V vs Fc}^{+/0}$) has been shown to involve two distinct processes occurring at -1.2 and -1.4 V , respectively.³⁶ On the basis of the acid concentration dependence of the voltammetric responses, it has been proposed that the less negative catalytic process is initiated by the N-protonation of the diiron dithiolate complex and is further limited by the slow release of H_2 from a $\{2\text{H}^+, 2\text{e}^-\}$ intermediate, whereas the most negative catalytic process corresponds to the fast H_2 release from a $\{3\text{H}^+, 3\text{e}^-\}$ intermediate. In addition, the potential at which occurs the more negative catalytic process seems to depend on the strength of the acid used as a proton source. Although voltammetry is a powerful technique to get information about dynamical electron and proton transfer processes, it gives little insight on the structure of the intermediate species involved in these processes. As a result, many details about the catalysis of electrochemical proton reduction by complexes of the type $[\text{Fe}_2(\mu\text{-SCH}_2\text{N}(\text{R})\text{CH}_2\text{S})(\text{CO})_6]$ remain elusive, impeding design of efficient catalysts inspired by FeFe– H_2 ase.

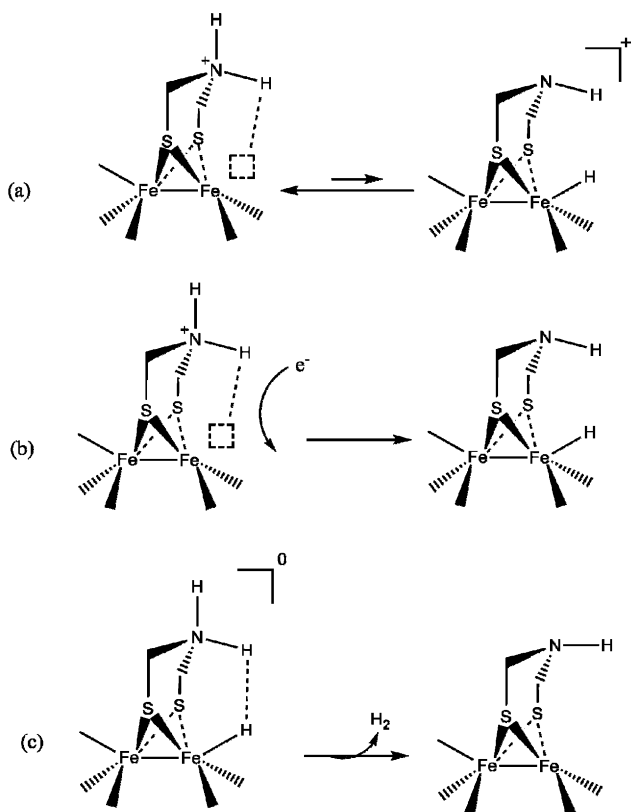
Received: July 28, 2014

Published: September 15, 2014

Scheme 1. Structure of the Active Site of [FeFe]-Hydrogenase (H cluster, dash bonds represent hydrogen bonds to the protein backbone) and Model Compounds Studied in the Present Work: Fe–adt, Fe–pdt, and Fe–bdt



Scheme 2. Possible Pathways Involving the Azadithiolate Bridge in Proton Reduction Catalysis by [FeFe]-H₂ase Models^a



^aOpen-dashed square represents an open coordination site.

We report here electrochemical and quantum chemistry studies of electron and proton transfer to the H₂ase model [Fe₂(μ-SCH₂N(H)CH₂S)(CO)₆] (Fe–adt) in acetonitrile. As previously reported with cobalt-based molecular catalysts for H₂ production,^{26,41} we use values of reduction potentials and pK_a estimated by density functional theory (DFT) calculation to rationalize the voltammetric responses recorded in the presence of proton sources of increasing strength. Then, analysis of the voltammetric responses under electrocatalytic conditions for Fe–adt,⁴² [Fe₂(μ-SCH₂CH₂CH₂S)(CO)₆] (Fe–pdt), and [Fe₂(μ-SC₆H₄S)(CO)₆] (Fe–bdt) is used to demonstrate the intrinsic catalytic effect of the adt bridge on the overall kinetics of proton reduction.

EXPERIMENTAL SECTION

[Fe₂(μ-SCH₂N(H)CH₂S)(CO)₆] (Fe–adt),⁴³ [Fe₂(μ-SCH₂CH₂CH₂S)(CO)₆] (Fe–pdt), and [Fe₂(μ-SC₆H₄S)(CO)₆] (Fe–bdt)⁴⁴ were prepared according to previously published procedures. Tetrabutylammonium hexafluorophosphate (Bu₄NPF₆) was purified by crystallization from methanol. Acetonitrile (MeCN, HPLC grade), *p*-toluenesulfonic acid monohydrate (HOTs·H₂O, pK_a = 8.6), trichloroacetic acid (CCl₃CO₂H, pK_a = 10.7), and chloroacetic acid (CClH₂CO₂H, pK_a = 15.3) were used as received.^{45–48}

Cyclic voltammetry (CV) experiments were carried out in N₂- or CO-purged 0.1 M Bu₄NPF₆/MeCN solutions, following the previously described procedure.^{39,49} The working electrode was a glassy carbon (GC) electrode of 0.071 cm² in surface area, polished prior to each experiment using alumina powder in water and then rinsed with acetone and dried. Ferrocene (Fc) was used as an internal standard added at the end of the experiments. Conversion of the potential scale against other reference electrodes is straightforward.⁵⁰ Background CVs of the acid in the absence of catalyst⁵¹ are shown in the Supporting Information.

DFT calculations were performed using the ORCA software package.⁵² Geometry optimization was carried out in the gas phase using the B3LYP⁵³ functional in combination with the def2-TZVP basis set for all atoms.⁵⁴ A corresponding effective core potential was applied to the Fe atoms.^{55,56} Vibrational analysis and single-point energy calculation were performed from the gas-phase-optimized geometry using the same functional and basis set, taking into account the effect of solvent using the conductor-like screening model (COSMO) for acetonitrile.⁵⁷ Calculations were accelerated with the resolution of identity and chain of sphere (RIJCOSX) approximations in conjunction with the def2-TZVP/J auxiliary basis set.^{58,59} Tight convergence criteria and increased integration grids were used. For ground states, vibrational analysis showed no imaginary components. Redox potentials and pK_a values were calculated using well-established thermodynamic cycles and corrected according to recently published procedures.⁶⁰ This approach has been shown to give accurate results for numerous molecular electrocatalysts.^{26,41,60–62}

RESULTS AND DISCUSSION

Voltammetry Studies and DFT Calculations. In the absence of proton source in solution, Fe–adt undergoes a two-electron reduction at $E_{1/2} = -1.58$ V (vs Fc⁺/Fc). Under CO atmosphere this reduction process becomes chemically reversible, indicating the occurrence of a follow up reaction in which CO loss is involved (see Supporting Information). The electrochemical behavior of Fe–adt in the absence of acid, which is very similar to that other complexes of the type [Fe₂(μ-SCH₂N(R)CH₂S)(CO)₆] (R ≠ H), will not be discussed in further detail here.

To calibrate our computational procedure, we calculated the reduction potential and pK_a value of Fe–adt in MeCN (Table 1). The calculated reduction potential of -1.60 V is in good

Table 1. Calculated and Experimental Reduction Potentials (E°) and pK_a Values in MeCN for Different Oxidation and Protonated States of Fe–adt Possibly Involved in Proton Reduction Catalysis

redox couple	E° (V vs Fc^+/Fc)		acid/base couple	pK_a
	calcd	exp		calcd
Fe–adt/Fe–adt [−] {0H ⁺ /1 e [−] }	−1.60	−1.58	Fe–adt–NH ⁺ /Fe–adt {1H ⁺ /0 e [−] }	8.2
Fe–adt–NH ⁺ /Fe–adt–NH ⁰ {1H ⁺ /1 e [−] }	−1.21	−1.27 ^{a,b}	Fe–adt–NH ⁰ /Fe–adt [−] {1H ⁺ /1 e [−] }	13.8
Fe–adt–Hyd ⁰ /Fe–adt–Hyd [−] {1H ⁺ /2 e [−] }	−1.68	−1.75 ^{a,c}	Fe–adt–Hyd ⁰ /Fe–adt [−] {1H ⁺ /1 e [−] }	17.1
Fe–adt–Hyd–NH ⁺ /Fe–adt–Hyd–NH ⁰ {2H ⁺ /2 e [−] }	−1.27	−1.40 ^{a,d}	Fe–adt–Hyd–NH ⁺ /Fe–adt–Hyd ⁰ {2H ⁺ /1 e [−] }	9.5
			Fe–adt–Hyd–NH ⁰ /Fe–adt–Hyd [−] {2H ⁺ /2 e [−] }	15.3

^a E_{pc} . ^bMeasured using 1.1 equiv of HOTs. ^cMeasured using 1.1 equiv of $ClCH_2COOH$. ^dEstimated using an excess of HOTs.

agreement with the experimental value. Moreover, the computed pK_a value of 8.2 for the protonated form Fe–adt–NH⁺ is in full agreement with the experimental value of 8.0 ± 0.2 previously measured by IR spectroscopy by Rauchfus and co-workers.⁶³

Fe–adt can readily react with acids that are strong enough to protonate the NH group ($pK_a < 8$). However, when the acid used as a proton source is comparatively weak, protonation of Fe–adt must be initiated by a reduction step as seen for Fe–pdt³² and Fe–bdt.⁶⁴ Here, addition of 1 mol equiv of $ClCH_2CO_2H$ ($pK_a = 15.3$) to a solution of Fe–adt in MeCN leads one to observe a complete irreversibility of the reduction peak of Fe–adt at -1.60 V associated with the appearance of a second reduction peak at $E_{pc} = -1.75$ V (Figure 1). Further

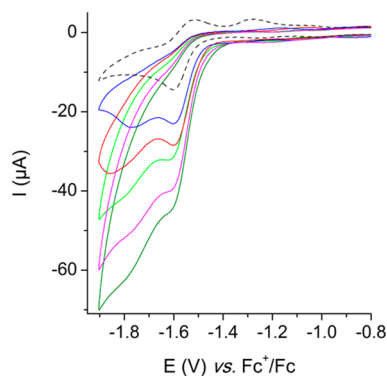


Figure 1. CVs of 0.5 mM Fe–adt in 0.1 M $Bu_4NPF_6/MeCN$ upon successive addition of $ClCH_2CO_2H$ ($pK_a = 15.3$): 0, 1, 2, 4, 6, and 8 mol equiv.

additions of $ClCH_2COOH$ trigger two catalytic proton reduction waves at potentials of ca. -1.60 and -1.75 V. Similarly, two catalytic proton reduction waves have been observed with Fe–pdt using HOTs in THF³² or with $[Fe_2(\mu-SCH_2N(R)CH_2S)(CO)_6]$ ($R = CH_2CH_2OCH_3$ ³⁶ or Ph ³⁷). At a concentration ratio $[acid]/[Fe-adt] = 8$, the ratio of the catalytic current (i_{cat}) to the peak current (i_p) in the absence of acid reaches a value of $i_{cat}/i_p \approx 3.1$ at -1.60 V and $i_{cat}/i_p \approx 4.2$ at -1.75 V.

$ClCH_2CO_2H$ is not acidic enough to protonate Fe–adt ($\Delta pK_a > 7$). However, since the reduction of diiron dithiolate

complexes enhances their basicity, the reduced form of Fe–adt is able to react with $ClCH_2CO_2H$. Indeed, DFT calculations show that both the nitrogen and the iron site of Fe–adt[−] are more basic than the NH site in neutral Fe–adt (Table 1). Moreover, the computed pK_a values are compatible with a protonation of Fe–adt[−] on the iron site ($pK_a = 17.1$) by $ClCH_2COOH$ ($pK_a = 15.3$) to give an intermediate bearing a terminal hydride (Fe–adt–Hyd⁰). The calculated reduction potential of Fe–adt–Hyd⁰ (-1.68 V) is in fair agreement with the experimental value of ca. -1.75 V. After reduction to Fe–adt–Hyd[−], the calculated pK_a of the NH site is ca. 15.3. The amine group is thus basic enough to allow further protonation by $ClCH_2COOH$, leading to the $\{2H^+/2 e^-\}$ species (Fe–adt–HydNH⁰). Furthermore, the distance of 1.45 Å between Fe–H and N–H in the optimized geometry is very short (Figure 2).

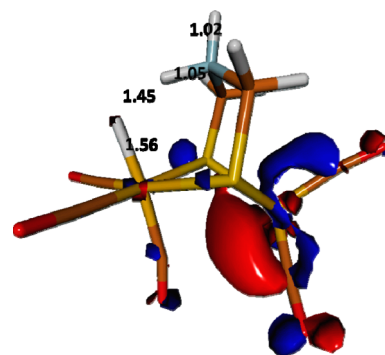
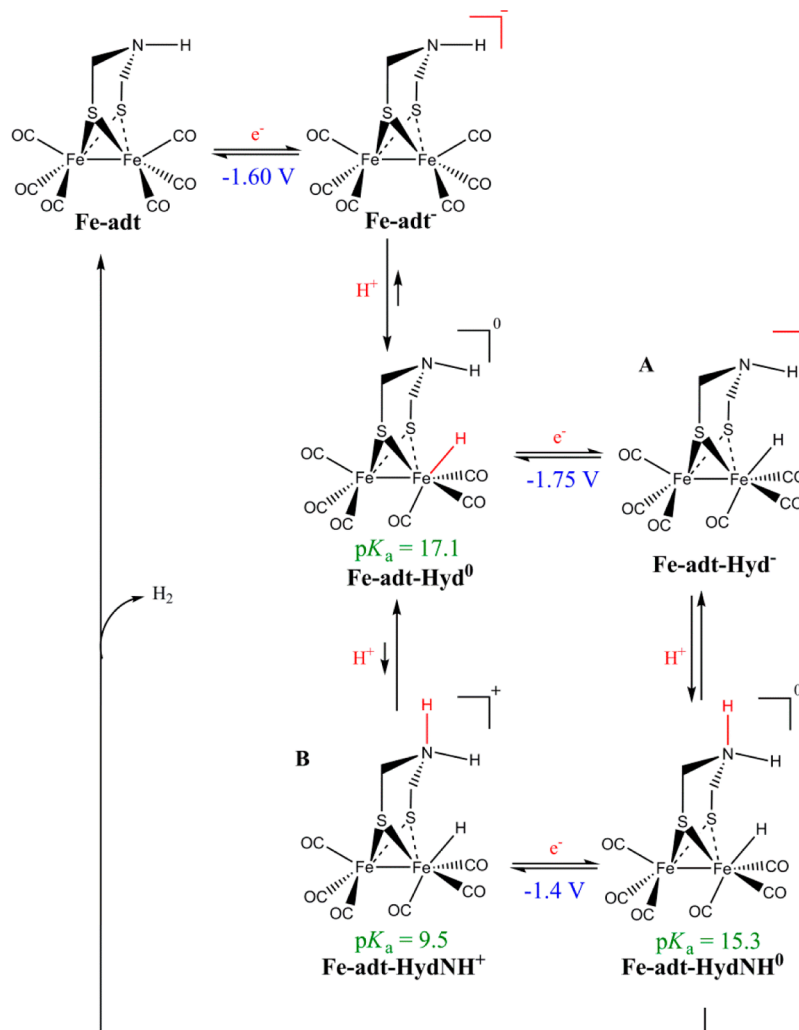


Figure 2. Optimized geometry of the $\{2H^+/2 e^-\}$ species Fe–adt–HydNH⁰, relevant interatomic distances (in Angstroms), and HOMO (highest occupied molecular orbital).

This result leads to the conclusion that there is a strong unconventional hydrogen bond between the two hydrogen atoms.^{21,22} Such an interaction would ease the release of H_2 regenerating Fe–adt, thus closing the catalytic cycle (Scheme 3, pathway A).

According to a similar reasoning, the observed catalytic proton reduction wave at -1.60 V would imply formation and subsequent reduction of the $\{2H^+/1 e^-\}$ species noted Fe–adt–HydNH⁺ (Scheme 3, pathway B). Nevertheless, considering the calculated pK_a value of the Fe–adt–HydNH⁺ ($pK_a = 9.5$), further protonation of Fe–adt–Hyd⁰ to Fe–adt–HydNH⁺ by $ClCH_2COOH$ seems unlikely ($\Delta pK_a \approx 6$). Since the proton transfer is very uphill, one might have to consider here a concerted proton–electron transfer, possibly coupled with formation and release of H_2 . This interesting phenomenon, for which detailed analysis is beyond the purpose of the present work, is currently under study in our lab.

As shown in Figure 3, addition of a few molar equivalents of CCl_3CO_2H ($pK_a = 10.7$) results in the appearance of a new reduction event at a potential of about -1.48 V, which is about 100 mV less negative than that of the primary reduction of Fe–adt. Since this new reduction event is observed at a potential less negative than primary reduction of Fe–adt and is responsive to the concentration of acid in solution it has to be ascribed to reduction of a protonated form of Fe–adt. Despite a difference of about 2.7 pK_a units between the acidity of the HNH⁺ group and that of CCl_3CO_2H , it is most probable that protonation of Fe–adt occurs at the NH group. As the concentration of Fe–adt–NH⁺ in the bulk solution is low (i.e., $[Fe-adt]/[Fe-adt-NH^+] \approx 20$ in the presence of 1 mol equiv

Scheme 3. Catalytic Cycles for Reduction of Proton Using ClCH_2COOH ($\text{p}K_a = 15.3$) as a Proton Source^a

^aRedox potentials are experimental measurements. Values of $\text{p}K_a$ were calculated by computational chemistry.

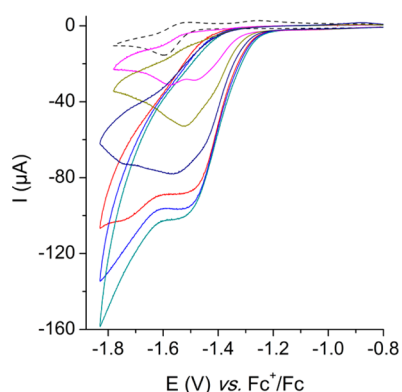


Figure 3. CVs of 0.5 mM Fe-adt in 0.1 M $\text{Bu}_4\text{NPF}_6/\text{MeCN}$ upon successive addition of $\text{Cl}_3\text{CCO}_2\text{H}$ ($\text{p}K_a = 10.7$): 0, 2, 4, 8, 12, 16, and 20 mol equiv.

of acid), this reduction process can be explained by the generation of Fe-adt-NH^+ in the vicinity of the electrode according to a CE mechanism. Then, the reduction step of the protonated form Fe-adt-NH^+ , at a potential less negative than Fe-adt , displaces the protonation equilibrium to the right.

The standard reduction potential of Fe-adt-NH^+ can be roughly estimated to be -1.32 V from the peak potential measured from a solution containing a few equivalents of $\text{Cl}_3\text{CCO}_2\text{H}$ (see Supporting Information). When using a stronger acid, such as HOTs ($\text{p}K_a = 8.6$), the effect of the fast pre-equilibrium protonation of Fe-adt on the voltammograms becomes negligible. Then a better estimate of -1.27 V for the reduction potential of Fe-adt-NH^+ is obtained (Figure 4). The discrepancy with the value estimated using $\text{Cl}_3\text{CCO}_2\text{H}$ as a proton source might be explained by the effect of a subsequent chemical reaction on the peak potential value. The calculated reduction potential of -1.21 V is in fair agreement with the experimental value of -1.27 V (Table 1).

With both $\text{Cl}_3\text{CCO}_2\text{H}$ and HOTs further additions of acid trigger broad catalytic proton reduction waves at the corresponding potential of the reduction of Fe-adt-NH^+ (ca. -1.48 and -1.27 V, respectively). At a concentration ratio $[\text{acid}]/[\text{Fe-adt}] = 12$, the current enhancement reaches a value of about $i_{\text{cat}}/i_p \approx 5$ for both acids. As explained above, for the reduced complex the diiron site is significantly more basic than the nitrogen site ($\Delta\text{p}K_a = 3.3$). Thus, subsequently to the electron transfer, Fe-adt-NH^0 might promptly undergo a tautomerization reaction, which leads to formation of Fe-adt-Hyd^0 . According to the calculated $\text{p}K_a$ value of 9.5, the nitrogen

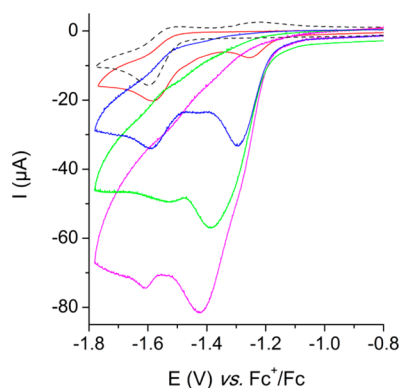


Figure 4. CVs of 0.5 mM Fe-adt in 0.1 M Bu₄NPF₆/MeCN upon successive addition of HOTs ($pK_a = 8.6$): 0, 1, 4, 8, and 12 mol equiv.

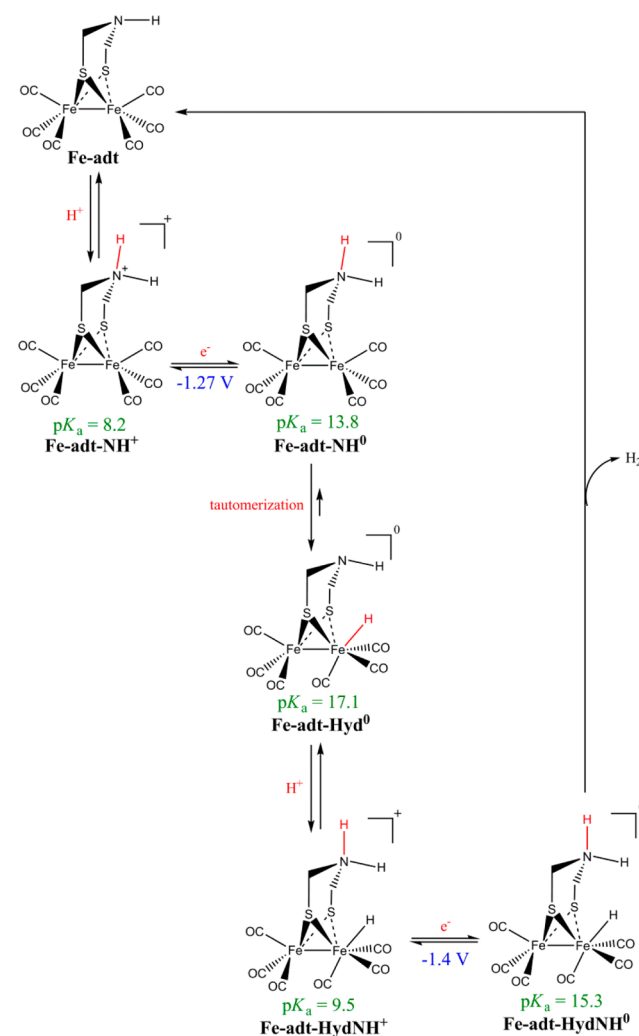
site of Fe-adt-Hyd⁰ is basic enough to be protonated either by Cl₃CCOOH or by HOTs. At the potential of the proton reduction catalytic wave (ca. -1.4 V), Fe-adt-HydNH⁺ ($E^{\circ}_{\text{calcd}} = -1.27$ V) is readily reduced. The resulting $\{2 \text{ H}^+/2 \text{ e}^-\}$ species Fe-adt-HydNH⁰ undergoes a loss of H₂, giving back Fe-adt, which closes the catalytic cycle (Scheme 4).

Foot-of-the-Wave Analysis under Electrocatalytic Conditions. Since we have shown that protonation of the NH group is fast on the CV time scale, we can assume that the catalysis of proton reduction by Fe-adt follows an EC_{cat} mechanism, in which the catalytic step C_{cat} is rate limiting. The pseudo-first-order rate constant k_{cat} (s⁻¹) of the catalytic step C_{cat} is often taken as a measure of the turnover frequency (TOF) of the catalyst. Note that here C_{cat} is not a single step but rather a succession of steps with one of them being rate determining. Savéant and co-workers recently proposed a method to extract the rate constant k_{cat} from CV experiments recorded under electrocatalytic conditions mixed with side phenomena, such as non-negligible substrate consumption or catalyst deactivation (Figure 5, see Supporting Information for detailed procedure and resulting plots).^{42,65} We previously applied this procedure to determine the TOF of Fe-bdt for catalysis of proton reduction in acetonitrile.⁴⁹

When the CV is not recorded in the acid-independent region, the pseudo-first-order rate constants calculated from the foot-of-wave analysis depend on the concentration of acid. Furthermore, the rate constant of the catalytic step is related to the overpotential $\eta = E_{1/2} - E^{\circ}_{\text{HA}/\text{H}_2}$ for the electrocatalytic reaction.⁶⁶ As a result, more meaningful data about the intrinsic efficiency of the electrocatalyst are obtained from second-order TOF at zero overpotential, noted TOF₀. The potential of the reduction of the proton depends on the pK_a of the acid: $E^{\circ}_{\text{HA}/\text{H}_2} = -0.76$ V for HOTs·H₂O, -0.88 V for CCl₃CO₂H, and -1.16 V for CH₂ClCO₂H.^{48,66} The kinetic parameters calculated for Fe-adt, Fe-pdt, and Fe-bdt are listed in Table 2.

Clearly, Fe-adt is intrinsically a much more efficient electrocatalyst than Fe-pdt or Fe-bdt independently of the acid being used as a proton source. To explain the better efficiency, two factors can be distinguished. First, protonation of the pendant base lowers the overpotential of the reduction of protons. Most likely, the reductions of the catalysts are then thermodynamically more accessible in the early stages of the catalysis. Second, the overall kinetics of the catalysis is faster for Fe-adt compared with Fe-pdt and Fe-bdt. The rate-limiting step of the catalysis, most likely formation and release of H₂, is

Scheme 4. Catalytic Cycle for the Reduction of Proton Using Moderately Strong Acid ($pK_a < 11$) as a Proton Source^a



^aRedox potentials are experimental peak potentials. pK_a values are calculated.

eased by the proximity between the HNH⁺ group and the FeH group in the later stages of the catalysis. The sum of these two factors leads to an intrinsically much more efficient electrocatalysis of the reduction of proton for the catalyst bearing a pendant base.

CONCLUSIONS

We report here a detailed electrochemical and quantum chemistry (DFT) study of electron and proton transfers to [Fe₂(μ-SCH₂NHCH₂S)(CO)₆] (Fe-adt) in MeCN solution. The electrochemical behavior of Fe-adt in the absence of acid was found to be very similar to that of other complexes of the type [Fe₂(μ-SCH₂N(R)CH₂S)(CO)₆] (R ≠ H). Our computational procedure was validated by a good agreement between the calculated and the experimental values of the reduction potential and pK_a of Fe-adt. Addition of moderately strong acids, such as CCl₃CO₂H ($pK_a = 10.7$) or HOTs·H₂O ($pK_a = 8.6$), triggers the occurrence of new reduction events at potentials less negative than the reduction of Fe-adt, therefore ascribed to reduction of protonated forms of the complex. The voltammetric responses in the presence of acid were rationalized by calculation of the structures, reduction

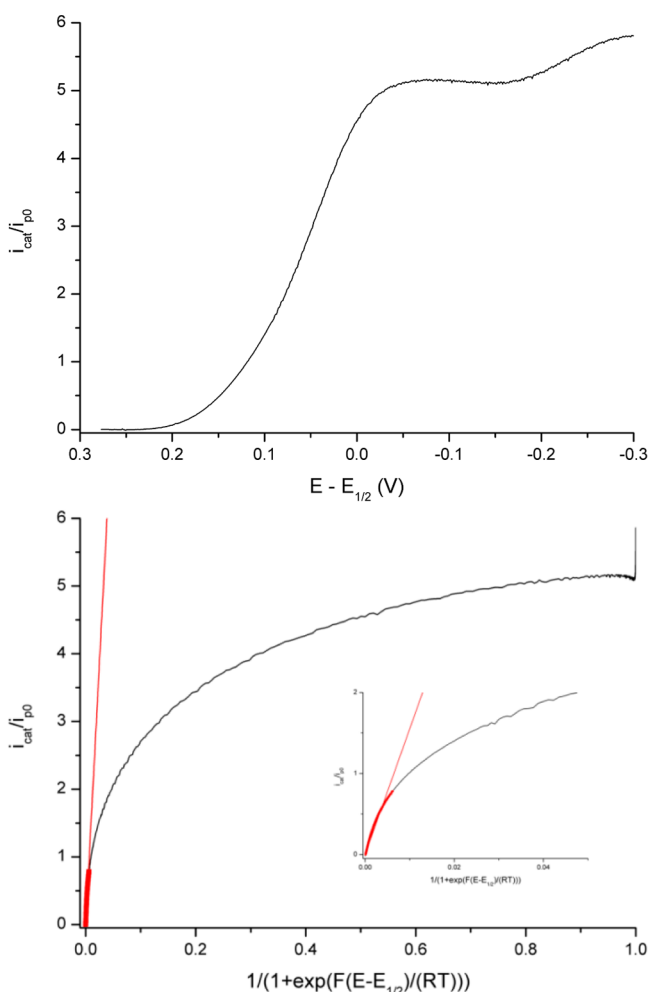


Figure 5. (Top) Background-corrected electrocatalytic response at $\nu = 0.1 \text{ V s}^{-1}$ of 0.5 mM Fe-adt in the presence of 12 mol equiv of $\text{CCl}_3\text{CO}_2\text{H}$. (Bottom) foot-of-the-wave analysis. Linear fit (red) to the data shows that the electrocatalytic responses deviate from ideal behavior at $i/i_p > 0.7$.

Table 2. Correlation between Pseudo-First-Order Rate Constant (k_{cat}), Second-Order Turnover Frequency at Zero Overpotential (TOF_0), and Overpotential (η) for the Proton Reduction Catalysts Studied Here

catalyst	acid	$ \eta $ (V)	$\log k_{\text{cat}}$ (s^{-1})	$\log \text{TOF}_0$ ($\text{M}^{-1} \text{s}^{-1}$)
Fe-adt	HOTs	0.86 ^a	3.0	-9.1
	Cl_3CCOOH	0.79 ^b	3.9	-7.0
	ClCH_2COOH	0.64 ^c	2.6	-5.8
Fe-pdt	HOTs	1.06	3.7	-11.8
	Cl_3CCOOH	0.94	3.1	-10.3
Fe-bdt ^{d9}	HOTs ^d	0.74	1.3	-11.1

^aConsidering $E = -1.4 \text{ V}$ for the potential of the catalysis.

^bConsidering $E = -1.45 \text{ V}$ for the potential of the catalysis, i.e., E_{pc} of the reduction of Fe-adt with few equivalents of Cl_3CCOOH

^cConsidering $E = -1.58 \text{ V}$ for the potential of the catalysis, i.e., reduction of Fe-adt ^dNo catalytic effect was observed at the potential of the first reduction with Fe-bdt using Cl_3CCOOH as an acid.

potentials, and $\text{p}K_{\text{a}}$ values of the reduced and protonated forms of Fe-adt. Interestingly, reduction of the N-protonated form seems to favor a tautomerization reaction leading to a putative Fe-H intermediate. Finally, the foot-of-the wave analysis of the CV responses of Fe-adt, $[\text{Fe}_2(\mu\text{-SCH}_2\text{CH}_2\text{CH}_2\text{S})(\text{CO})_6]$

(Fe-pdt), and $[\text{Fe}_2(\mu\text{-SC}_6\text{H}_4\text{S})(\text{CO})_6]$ (Fe-bdt) under electrocatalytic conditions demonstrated the intrinsic catalytic effect of the adt bridge on the overall kinetics of proton reduction.

■ ASSOCIATED CONTENT

📄 Supporting Information

Detailed procedures for the foot-of-the-wave analysis and estimation of peak potentials of protonated species, cyclic voltammetry under CO atmosphere; optimized structures, coordinates, calculated $\text{p}K_{\text{a}}$, and reduction potential of Fe-adt, Fe-adt⁻, Fe-adt-SH⁺ (protonated on one sulfur atom), Fe-adt-SH⁰, Fe-adt-NH⁺, Fe-adt-NH⁰, Fe-adt- μHyd^+ (bridging hydride), Fe-adt- μHyd^0 , Fe-adt- μHyd^- , Fe-adt-Hyd⁺, Fe-adt-Hyd⁰, Fe-adt-Hyd⁻, and Fe-adt-HydNH⁺. This material is available free of charge via the Internet at <http://pubs.acs.org>.

■ AUTHOR INFORMATION

Corresponding Authors

*E-mail: marc.bourrez@univ-brest.fr.

*E-mail: fgloague@univ-brest.fr.

Notes

The authors declare no competing financial interest.

■ ACKNOWLEDGMENTS

This work was supported by the Agence Nationale de la Recherche (ANR, BLANC SIMI9/0926-1, "TechBioPhyp"), the Centre National de la Recherche Scientifique (CNRS), and the Université de Bretagne Occidentale (UBO). We thank Prof. Rauchfuss at UIUC for the generous gift of Fe-adt.

■ REFERENCES

- (1) Nocera, D. G. *Acc. Chem. Res.* **2012**, *45*, 767–776.
- (2) Du, P.; Eisenberg, R. *Energy Environ. Sci.* **2012**, *5*, 6012–6021.
- (3) Wang, M.; Chen, L.; Sun, L. *Energy Environ. Sci.* **2012**, *5*, 6763–6778.
- (4) Omae, I. *Catal. Today* **2006**, *115*, 33–52.
- (5) Omae, I. *Coord. Chem. Rev.* **2012**, *256*, 1384–1405.
- (6) Adesina, A. A. *Appl. Catal. A-Gen.* **1996**, *138*, 345–367.
- (7) Dry, M. E. *Catal. Today* **2002**, *71*, 227–241.
- (8) Morris, A. J.; Meyer, G. J.; Fujita, E. *Acc. Chem. Res.* **2009**, *42*, 1983–1994.
- (9) Costentin, C.; Robert, M.; Savéant, J.-M. *Chem. Soc. Rev.* **2013**, *42*, 2423.
- (10) Qiao, J.; Liu, Y.; Hong, F.; Zhang, J. *Chem. Soc. Rev.* **2014**, *43*, 631.
- (11) Kondratenko, E. V.; Mul, G.; Baltrusaitis, J.; Larrazábal, G. O.; Pérez-Ramírez, J. *Energy Environ. Sci.* **2013**, *6*, 3112.
- (12) Kumar, B.; Llorente, M.; Froehlich, J.; Dang, T.; Sathrum, A.; Kubiak, C. P. *Annu. Rev. Phys. Chem.* **2012**, *63*, 541–569.
- (13) Vignais, P. M.; Billoud, B. *Chem. Rev.* **2007**, *107*, 4206–4272.
- (14) Lubitz, W.; Ogata, H.; Rüdiger, O.; Reijerse, E. *Chem. Rev.* **2014**, *114*, 4081–4148.
- (15) Peters, J. W. *Science* **1998**, *282*, 1853–1858.
- (16) Nicolet, Y.; Piras, C.; Legrand, P.; Hatchikian, C. E.; Fontecilla-Camps, J. C. *Structure* **1999**, *7*, 13–23.
- (17) Schilter, D.; Rauchfuss, T. B. *Angew. Chem., Int. Ed.* **2013**, *52*, 13518–13520.
- (18) Nicolet, Y.; de Lacey, A. L.; Vernède, X.; Fernandez, V. M.; Hatchikian, C. E.; Fontecilla-Camps, J. C. *J. Am. Chem. Soc.* **2001**, *123*, 1596–1601.
- (19) Silakov, A.; Wenk, B.; Reijerse, E.; Lubitz, W. *Phys. Chem. Chem. Phys.* **2009**, *11*, 6592.

- (20) Berggren, G.; Adamska, A.; Lambertz, C.; Simmons, T. R.; Esselborn, J.; Atta, M.; Gambarelli, S.; Mouesca, J.-M.; Reijerse, E.; Lubitz, W.; Happe, T.; Artero, V.; Fontecave, M. *Nature* **2013**, *499*, 66–69.
- (21) Belkova, N. V.; Shubina, E. S.; Epstein, L. M. *Acc. Chem. Res.* **2005**, *38*, 624–631.
- (22) Besora, M.; Lledós, A.; Maseras, F. *Chem. Soc. Rev.* **2009**, *38*, 957.
- (23) Liu, T.; Wang, X.; Hoffmann, C.; DuBois, D. L.; Bullock, R. M. *Angew. Chem., Int. Ed.* **2014**, *53*, 5300–5304.
- (24) Mayer, J. M. *Annu. Rev. Phys. Chem.* **2004**, *55*, 363–390.
- (25) Weinberg, D. R.; Gagliardi, C. J.; Hull, J. F.; Murphy, C. F.; Kent, C. A.; Westlake, B. C.; Paul, A.; Ess, D. H.; McCafferty, D. G.; Meyer, T. J. *Chem. Rev.* **2012**, *112*, 4016–4093.
- (26) Solis, B. H.; Hammes-Schiffer, S. *Inorg. Chem.* **2014**, *53*, 6427–6443.
- (27) Costentin, C.; Robert, M.; Savéant, J.-M.; Tard, C. *Acc. Chem. Res.* **2014**, *47*, 271–280.
- (28) Gloaguen, F.; Rauchfuss, T. B. *Chem. Soc. Rev.* **2009**, *38*, 100–108.
- (29) Tschierlei, S.; Ott, S.; Lomoth, R. *Energy Environ. Sci.* **2011**, *4*, 2340.
- (30) Capon, J.-F.; Gloaguen, F.; Pétilion, F. Y.; Schollhammer, P.; Talarmin, J. *Coord. Chem. Rev.* **2009**, *253*, 1476–1494.
- (31) Felton, G. A. N.; Mebi, C. A.; Petro, B. J.; Vannucci, A. K.; Evans, D. H.; Glass, R. S.; Lichtenberger, D. L. *J. Organomet. Chem.* **2009**, *694*, 2681–2699.
- (32) Borg, S. J.; Behrsing, T.; Best, S. P.; Razavet, M.; Liu, X.; Pickett, C. J. *J. Am. Chem. Soc.* **2004**, *126*, 16988–16999.
- (33) Chong, D.; Georgakaki, I. P.; Mejia-Rodriguez, R.; Sanabria-Chinchilla, J.; Soriaga, M. P.; Daresbourg, M. Y. *Dalton Trans.* **2003**, 4158–4163.
- (34) Wang, N.; Wang, M.; Chen, L.; Sun, L. *Dalton Trans.* **2013**, *42*, 12059.
- (35) Lounissi, S.; Zampella, G.; Capon, J.-F.; De Gioia, L.; Matoussi, F.; Mahfoudhi, S.; Pétilion, F. Y.; Schollhammer, P.; Talarmin, J. *Chem.—Eur. J.* **2012**, *18*, 11123–11138.
- (36) Capon, J.-F.; Ezzaher, S.; Gloaguen, F.; Pétilion, F. Y.; Schollhammer, P.; Talarmin, J. *Chem.—Eur. J.* **2008**, *14*, 1954–1964.
- (37) Ott, S.; Kritikos, M.; Åkermark, B.; Sun, L.; Lomoth, R. *Angew. Chem., Int. Ed.* **2004**, *43*, 1006–1009.
- (38) Eilers, G.; Schwartz, L.; Stein, M.; Zampella, G.; de Gioia, L.; Ott, S.; Lomoth, R. *Chem.—Eur. J.* **2007**, *13*, 7075–7084.
- (39) Ezzaher, S.; Capon, J.-F.; Gloaguen, F.; Pétilion, F. Y.; Schollhammer, P.; Talarmin, J. *Inorg. Chem.* **2007**, *46*, 9863–9872.
- (40) Carroll, M. E.; Barton, B. E.; Rauchfuss, T. B.; Carroll, P. J. *J. Am. Chem. Soc.* **2012**, *134*, 18843–18852.
- (41) Solis, B. H.; Hammes-Schiffer, S. *Inorg. Chem.* **2011**, *50*, 11252–11262.
- (42) Costentin, C.; Drouet, S.; Robert, M.; Savéant, J.-M. *J. Am. Chem. Soc.* **2012**, *134*, 11235–11242.
- (43) Stanley, J. L.; Rauchfuss, T. B.; Wilson, S. R. *Organometallics* **2007**, *26*, 1907–1911.
- (44) Capon, J.-F.; Gloaguen, F.; Schollhammer, P.; Talarmin, J. *J. Electroanal. Chem.* **2004**, *566*, 241–247.
- (45) Eckert, F.; Leito, I.; Kaljurand, I.; Kütt, A.; Klamt, A.; Diedenhofen, M. *J. Comput. Chem.* **2009**, *30*, 799–810.
- (46) Kütt, A.; Rodima, T.; Saame, J.; Raamat, E.; Mäemets, V.; Kaljurand, I.; Koppel, I. A.; Garlyauskayte, R. Y.; Yagupolskii, Y. L.; Yagupolskii, L. M.; Bernhardt, E.; Willner, H.; Leito, I. *J. Org. Chem.* **2011**, *76*, 391–395.
- (47) Raamat, E.; Kaupmees, K.; Ovsjannikov, G.; Trummal, A.; Kütt, A.; Saame, J.; Koppel, I.; Kaljurand, I.; Lipping, L.; Rodima, T.; Pihl, V.; Koppel, I. A.; Leito, I. *J. Phys. Org. Chem.* **2013**, *26*, 162–170.
- (48) Felton, G. A. N.; Glass, R. S.; Lichtenberger, D. L.; Evans, D. H. *Inorg. Chem.* **2006**, *45*, 9181–9184.
- (49) Quentel, F.; Gloaguen, F. *Electrochim. Acta* **2013**, *110*, 641–645.
- (50) Pavlishchuk, V. V.; Addison, A. W. *Inorg. Chim. Acta* **2000**, *298*, 97–102.
- (51) McCarthy, B. D.; Martin, D. J.; Rountree, E. S.; Ullman, A. C.; Dempsey, J. L. *Inorg. Chem.* **2014**, *53*, 8350–8361.
- (52) Neese, F. *Wiley Interdiscip. Rev. Comput. Mol. Sci.* **2012**, *2*, 73–78.
- (53) Lee, C.; Yang, W.; Parr, R. G. *Phys. Rev. B* **1988**, *37*, 785–789.
- (54) Weigend, F.; Ahlrichs, R. *Phys. Chem. Chem. Phys.* **2005**, *7*, 3297.
- (55) Dolg, M.; Wedig, U.; Stoll, H.; Preuss, H. *J. Chem. Phys.* **1987**, *86*, 866.
- (56) Martin, J. M. L.; Sundermann, A. *J. Chem. Phys.* **2001**, *114*, 3408.
- (57) Klamt, A.; Schürmann, G. *J. Chem. Soc., Perkin Trans. 2* **1993**, 799.
- (58) Izsák, R.; Neese, F.; Klopper, W. *J. Chem. Phys.* **2013**, *139*, 094111.
- (59) Kossmann, S.; Neese, F. *Chem. Phys. Lett.* **2009**, *481*, 240–243.
- (60) Keith, J. A.; Grice, K. A.; Kubiak, C. P.; Carter, E. A. *J. Am. Chem. Soc.* **2013**, *135*, 15823–15829.
- (61) Kelly, C. P.; Cramer, C. J.; Truhlar, D. G. *J. Phys. Chem. B* **2006**, *110*, 16066–16081.
- (62) Song, J.; Klein, E. L.; Neese, F.; Ye, S. *Inorg. Chem.* **2014**, *53*, 7500–7507.
- (63) Stanley, J. L.; Heiden, Z. M.; Rauchfuss, T. B.; Wilson, S. R.; De Gioia, L.; Zampella, G. *Organometallics* **2008**, *27*, 119–125.
- (64) Felton, G. A. N.; Vannucci, A. K.; Chen, J.; Lockett, L. T.; Okumura, N.; Petro, B. J.; Zakai, U. I.; Evans, D. H.; Glass, R. S.; Lichtenberger, D. L. *J. Am. Chem. Soc.* **2007**, *129*, 12521–12530.
- (65) Costentin, C.; Savéant, J.-M. *ChemElectroChem* **2014**, *1*, 1226–1236.
- (66) Roberts, J. A. S.; Bullock, R. M. *Inorg. Chem.* **2013**, *52*, 3823–3835.